J Mater Sci

Chemical routes to materials

Role of precursor type and thermal treatment in shaping the surface and colloidal properties of cadmium yellow pigments

Magdalena Tworek[1,*], Edwin Makarewicz[1], Magdalena Osial[2], Joanna Kowalik[1], and Magdalena Warczak[1]

[1] *Faculty of Chemical Engineering and Technology, Bydgoszcz University of Science and Technology, Seminaryjna 3, 85-326 Bydgoszcz, Poland*

[2] *Institute of Fundamental Technological Research, Polish Academy of Sciences, Pawińskiego 5B, 02-106 Warsaw, Poland*

Received: 1 December 2025
Accepted: 3 April 2026

ABSTRACT

This study presents the results of investigations on the influence of raw material type and synthesis method of cadmium yellow on the electrokinetic potential of pigment particles and the sedimentation stability of the resulting dispersions in various chemical environments. Pigments were synthesized from cadmium salts (chloride, sulfate, nitrate, and carbonate) using sodium sulfide or elemental sulfur as sulfur sources. Two synthesis routes were applied: (1) precipitation of the pigment from solution, followed by filtration, drying at 60 °C, and calcination at 600 °C in acidic and alkaline media; and (2) direct reaction of cadmium carbonate with sulfur at 600 °C. The materials were characterized using Raman spectroscopy and X-ray photoelectron spectroscopy (XPS). The zeta potential of the particles was measured at different pH values, and dispersion stability was evaluated by turbidimetric analysis (Turbiscan). The obtained pigments were mixtures of compounds, with cadmium sulfide (CdS) being the predominant component. The chemical composition depended on the synthesis route and the calcination process. A correlation was found between the electrokinetic potential, sedimentation stability, and chemical composition of the pigments. Calcination significantly affected surface properties, while the presence of chloride, sulfite, sulfate, and carbonate species modified the electrokinetic potential. Acidic environments were found to enhance the sedimentation stability of cadmium-based pigments. The findings highlight the importance of synthesis conditions for the surface chemistry, electrokinetic behavior, and sedimentation stability of cadmium-based pigments in aqueous systems.

Handling Editor: Subodh Ganesanpotti.

Address correspondence to E-mail: m.tworek@pbs.edu.pl

https://doi.org/10.1007/s10853-026-12724-w
Published online: 14 April 2026

GRAPHICAL ABSTRACT

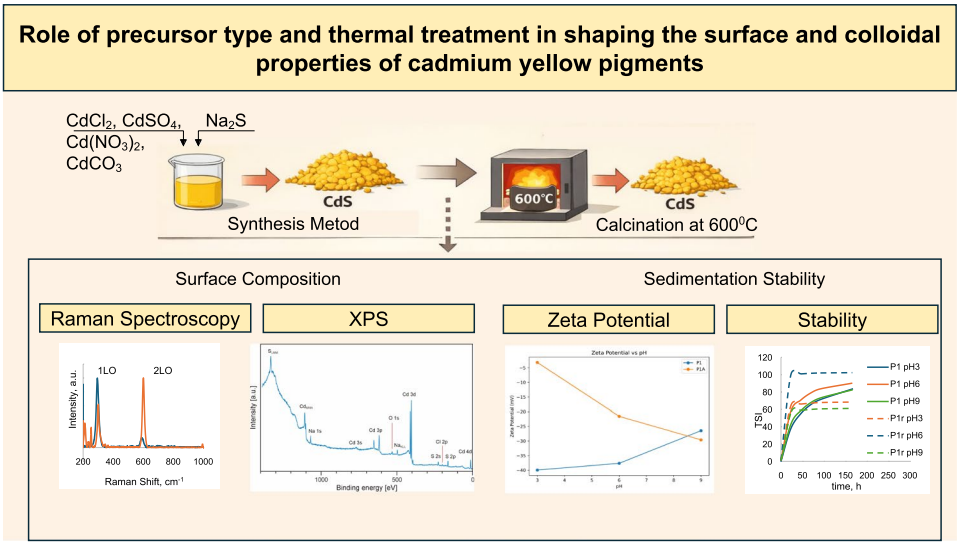

Introduction

Inorganic pigments and mineral fillers have a significant influence on the physical, mechanical, chemical, and thermal properties of polymeric materials. In many cases, they reinforce the structure of the material, improving its resistance to mechanical damage and environmental factors [1, 2]. One of the most important characteristics of pigments is their behavior under solar radiation and in liquid or solid media. The surface activity of pigments involves adsorption phenomena of dissolved substances that can form a new phase at the interface, thus affecting the stability of dispersion systems. Such processes are often related to the presence of surface-active agents. The surface properties of pigments depend on their chemical composition, crystal structure, synthesis method, thermal treatment, and storage conditions [3–5].

An essential factor determining the stability of pigment dispersions is the electrokinetic potential (ζ-potential), which reflects the surface charge of pigment particles at the phase boundary. A high absolute ζ-potential promotes electrostatic repulsion between particles, limiting coagulation and enhancing dispersion stability. The value of the ζ-potential depends on the pigment composition, the type of ions present in the solution, the pH, and the nature of the particle surface [6]. Adsorption of dissolved substances may further modify the surface tension and lead to the formation of stabilizing adsorption layers, reducing sedimentation and aggregation tendencies [7–9]. The overall stability of such dispersions is governed by coagulation, flocculation, and separation processes.

Numerous studies have demonstrated that surface modification of cadmium pigments, for example by silica or organic coatings, markedly improves their chemical stability and resistance to photodegradation [10]. Investigations of CdS, CdSe, and CdS–SiO_2 systems have confirmed the key role of surface structure and composition in determining their durability and optoelectronic properties. In contrast, photodegradation of cadmium yellow and cadmium red pigments leads to oxidation of sulfur to sulfate forms and to the release of cadmium ions into the environment [11–16]. The presence of organic matter, such as humic acids, can affect the aggregation and stability of CdS nanoparticles in electrolyte solutions [17, 18]. Other studies have identified secondary degradation products—such as cadmium carbonates, oxalates, and sulfates—within aged paint layers containing cadmium pigments [19–21]. Enhanced pigment stability can be achieved by coating CdS particles with silica or by thermal treatment in the presence of in situ carbon, yielding bright, saturated colors and reducing cadmium solubility [22, 23].

Despite extensive research on cadmium pigments, most previous studies have focused either on their

optical properties, degradation processes, or environmental behavior. Comparatively less attention has been paid to the relationship between synthesis conditions, surface chemical composition, electrokinetic properties, and the stability of pigment dispersions in aqueous systems. In particular, systematic studies combining structural characterization with electrokinetic measurements and sedimentation analysis remain limited. A comprehensive understanding of how synthesis pathways and thermal treatment influence surface chemistry and, consequently, the electrokinetic behavior and dispersion stability of CdS pigments is still lacking.

The aim of this study was to determine the effect of the type of precursors and the synthesis method of cadmium sulfide yellow pigment on the electrokinetic potential of its particles and the stability of aqueous dispersions formed from them. Laboratory syntheses of cadmium yellow were carried out using two different approaches: (1) precipitation from solution followed by drying and calcination, and (2) reaction in the molten state at elevated temperature between homogeneously mixed solid substrates. The obtained pigments were finely ground and homogenized and subsequently characterized using Raman spectroscopy, X-ray photoelectron spectroscopy (XPS), electrokinetic measurements, and sedimentation analysis. The interpretation of the results focused on identifying the relationships between synthesis conditions, surface composition, and physicochemical properties of the pigments.

Experimental part

Materials

The following chemical reagents were used to synthesize the pigments:

- Sodium sulfide ($Na_2S{\cdot}9H_2O$, ≥ 98% purity, Merck Life Science Sp. z o.o.) with a decomposition temperature of 120 °C,
- Cadmium chloride ($CdCl_2{\cdot}2H_2O$, ≥ 99% purity, Merck Life Science Sp. z o.o.) with a melting point of 565 °C and a boiling point of 964 °C,
- Cadmium sulfate ($CdSO_4{\cdot}8H_2O$, ≥ 99% purity, Merck Life Science Sp. z o.o.) with a melting point of 41 °C and a decomposition temperature above 80 °C,
- Cadmium nitrate ($Cd(NO_3)_2{\cdot}4H_2O$, ≥ 99% purity, Merck Life Science Sp. z o.o.) with a melting point of 59 °C and a boiling point of 350 °C,
- Cadmium carbonate ($CdCO_3$, ≥ 99% purity, Merck Life Science Sp. z o.o.) with a melting point of 343 °C and a decomposition temperature of 412 °C,
- Sulfur (S, ≥ 99.5% purity, Merck Life Science Sp. z o.o.) with a melting point of 115 °C and a boiling point of 444.61 °C.

The pH of the solutions was adjusted using concentrated sulfuric acid (H_2SO_4, 95–98% purity, Merck Life Science Sp. z o.o.). The industrial cadmium pigment with the trade name cadmium yellow ST supplied by Zakłady Chemiczne Permedia SA in Lublin (Poland) was additionally purified by extraction with ethyl acetate.

Methods

Preparation of cadmium yellow

Cadmium yellow was obtained by two methods, i.e. precipitation from solution according to reaction Eqs. (1)–(4) and melting according to reaction Eq. (5):

$$CdCl_2 + Na_2S = CdS + 2NaCl \quad (1)$$

$$CdSO_4 + Na_2S = CdS + Na_2SO_4 \quad (2)$$

$$Cd(NO_3)_2 + Na_2S = CdS + 2NaNO_3 \quad (3)$$

$$CdCO_3 + Na_2S = CdS + Na_2CO_3 \quad (4)$$

$$2CdCO_3 + 3S = 2CdS + 2CO_2 + SO_2 \quad (5)$$

Table 1 presents the proposed compositions of samples prepared for the pigment syntheses. The calculations included 0.1 mol of starting substrates.

Two synthesis routes were employed to obtain cadmium yellow (CdS) pigment.

In the first method, CdS was precipitated from aqueous substrate solutions (quantities listed in Table 1). The precipitation was carried out in a 500 cm^3 beaker at 90–98 °C for 1h. Upon completion, the pH of the reaction medium was approximately 12. To remove residual reactive Na_2S and stabilize the precipitate, the suspension of sample P2 was acidified with concentrated sulfuric acid to a pH of 1–2. The pigment

Table 1 Designations and initial compositions of test samples

Pigment designation	Qualitative and quantitative compositions of reaction mixtures			Preparation method	pH
	Cd	S	H_2O, cm^3		
P1	$CdCl_2{\cdot}2H_2O$, 5.7 g	$Na_2S{\cdot}9H_2O$, 6.0 g	400	Precipitation	12
P2	$CdCl_2{\cdot}2H_2O$, 5.7 g	$Na_2S{\cdot}9H_2O$, 6.0 g	400	Precipitation	1–2
P3	$CdSO_4{\cdot}8H_2O$, 8.8 g	$Na_2S{\cdot}9H_2O$, 6.0 g	400	Precipitation	12
P4	$Cd(NO_3)_2{\cdot}4H_2O$; 7, 7 g	$Na_2S{\cdot}9H_2O$ 6.0 g	400	Precipitation	12
P5	$CdCO_3$, 4.3 g	$Na_2S{\cdot}9H_2O$, 6.0 g	400	Precipitation	12
P6	$CdCO_3$, 3.44 g	S; 0.96 g	–	Melting	–
P7	Industrial pigment-cadmium yellow ST			–	–

suspensions were then cooled to room temperature, filtered, and washed with distilled water until neutral pH was achieved (five washings, 50 cm^3 each). The obtained wet pigments were dried at 100 °C for 24h in a forced-air oven, followed by gentle grinding and homogenization in a porcelain mortar to obtain uniform powders for further analyses.

In the second method, cadmium yellow was synthesized by solid-state roasting. The previously prepared pigment samples were placed in closed porcelain crucibles and calcined in a muffle furnace at 600 °C for 1.5h. After cooling to room temperature, the pigments were crushed and homogenized in a porcelain mortar.

Additionally, CdS was synthesized directly by fusion of cadmium carbonate and sulfur in closed porcelain crucibles under the same conditions (600 °C, 1.5 h). The obtained products were similarly cooled, ground, and homogenized.

All pigments prepared by both precipitation and solid-state fusion methods were subjected to further physicochemical and structural characterization.

Preparation dispersion of cadmium yellow

To prepare aqueous pigment dispersions, 0.3 g of CdS powder was weighed and transferred to a beaker, to which 30 mL of deionized water was added. The resulting suspension was dispersed for approximately 1–2 min in an IKA-ULTRA-TURRAX T25 laboratory homogenizer with an S25 N-18 Gz stirrer at 1500 rpm. The pH of the samples was adjusted using acetic acid (for acidic environments) or NaOH solution (for alkaline environments), obtaining the required pH values (3, 6, and 9). After pH adjustment, the dispersions were briefly mixed again and subjected to further testing.

Methodology

Raman spectroscopy

The spectra were made using Raman microscopy using a Bruker Raman II Optik Senterra GmbH spectrometer equipped with a laser with a wavelength of 532 nm and a power of 2.5 mW. The aperture was set to 50 μm, and the microscope objective magnification was 20 × . All samples were round tablets with a diameter of 1.0 cm and a mass of 700 mg. Measurements were performed using the point method. At one freely selected point, 20 scans were performed in 10s.

Electrokinetic potential

The Zeta potential (ζ) measurements were performed using Zetasizer Nano ZS supplied from the Malvern Instruments, Malvern, UK. Measurements were performed in the disposable cuvette under the controlled pH as follows pH 3, pH 6, and pH 9, with the CdS concentration about 0.2 mg/mL. Prior to the measurements, each powder-like sample was ground using a mortar and pestle and then, vortexed for 1 min and followingly sonicated for 10 min. ζ values were reported as the result of technical repetitions (five consecutive measurements) of the same dispersion; independent dispersion preparations were not performed, therefore reproducibility between preparations was not assessed.

XPS photoelectron spectroscopy

XPS photoelectron spectra were recorded under ultrahigh vacuum conditions (base pressure in the analyzer chamber was ≤ 2·10–10 mbar). The source of monochromatic excitation radiation was an AlKα lamp with an energy of 1486.6 eV. The X-ray beam angle to the sample surface normal was 55°. The energy of photoelectrons emitted from the sample surfaces was recorded using a VG-Scienta R3000 hemispherical analyzer. The major axis of the analyzer was oriented perpendicular to the sample surface. High-resolution spectra from individual sample regions were recorded with a $\Delta E = 100$ meV step. After modeling a Shirley-type background, all experimental data were fitted to Gaussian–Lorentzian curves using Casa XPS software. The research results were interpreted based on the data presented in [24–28].

The principle of Turbiscan LAB measurement

Turbiscan LAB was employed to quantitatively and objectively characterize the stability of dispersion system samples without destruction, to avoid the interference of subjective factors and to show the cause of instability [29].

The analyzed emulsion was placed in a cylindrical measuring glass cell. The optical reading head scanned the length of the sample (55 mm) acquiring backscattering data as a function of the distance along the axis of the tube and time (transmitted light was neglected because the emulsion is opaque). Backscattered light (BS) and Turbiscan Stability Index (TSI) are used to quantify the stability of samples. The calculation method of this coefficient is as follows:

$$\mathrm{TSI} = \sqrt{\frac{\sum_{i=1}^{N} \left(x_i - x_{\mathrm{m}}\right)^2}{N-1}} \tag{6}$$

where x_i ($i = 1,\ldots, N$) is the mean backscattering, x_{m} is the mean value of x_i, and N is the number of scans. The smaller the TSI value, the more stable the sample. The measurement was performed on the day of sample preparation and then after 7, 14 and 21 days of exposure at 20 ± 1 °C.

Statistical correlation analysis

Correlation analysis was performed using the Pearson correlation coefficient (r) and the Spearman rank correlation coefficient (ρ), along with p-values (two-tailed test). Correlations were calculated separately for pH 3, 6, and 9. The correlation coefficient, p-value, and number of observations (N) are reported.

Results

Raman characterization of cadmium yellow

Raman spectroscopy was used to evaluate the qualitative composition and degree of structural order of cadmium yellow pigments obtained by precipitation and solid-state synthesis. Figure 1 presents the Raman spectra of pigments obtained from various cadmium precursors and sulfur sources, before and after calcination at 600 °C.

In all samples, characteristic CdS bands are observed: 1LO at ~ 300–305 cm^{-1} and 2LO at ~ 600–610 cm^{-1}, confirming that CdS is the dominant component. Some spectra also exhibit weak signals at higher shifts (~ 900–1000 cm^{-1}), where a 3LO contribution may occur. The presence of these additional bands may indicate secondary surface species and/or a greater contribution of structural disorder; however, Raman spectroscopy alone does not allow for unambiguous identification of crystalline impurity phases. Calcination typically leads to narrowing and better development of the LO bands and—in selected samples—to a more pronounced higher-order bands, indicating increased order/crystallinity. In some cases, additional weak bands appear after calcination, suggesting modification/oxidation of the surface layer, consistent with the HR-XPS results (presence of oxidized sulfur species). Precipitation samples typically exhibit broader LO bands and a stronger contribution of low-frequency signals (higher defect content), whereas the solid-state sample (P6) and the industrial pigment (P7) exhibit more pronounced higher-order phonon features (e.g., 3LO), indicating higher crystallinity. In summary, Raman confirms the formation of CdS in all variants, and differences in band shape and

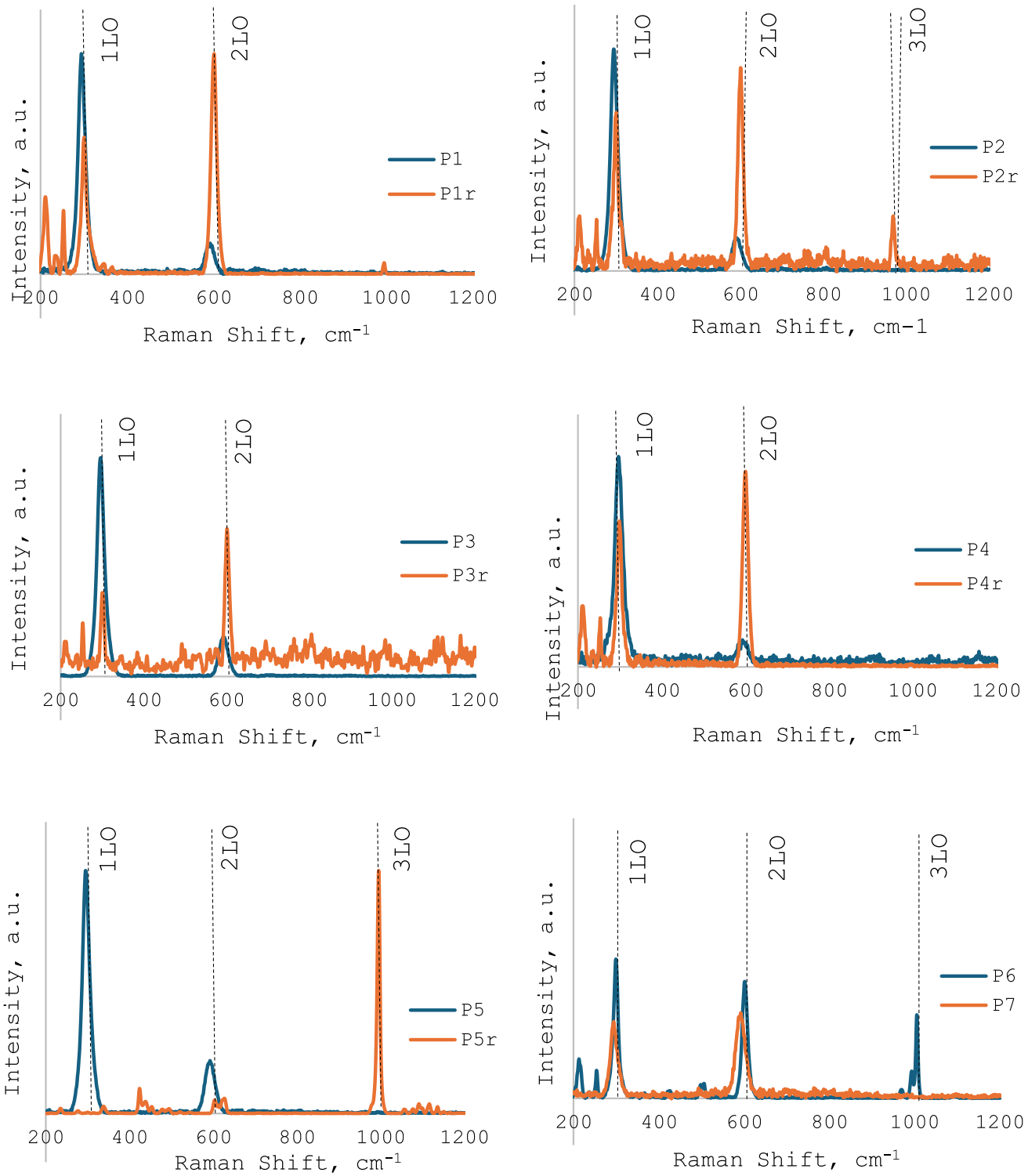

Figure 1 Raman spectra of CdS pigments after precipitation and drying, and after calcination. Pigment types are indicated according to Table 1; the letter "*r*" denotes calcined pigments.

Table 2 Surface potential values of cadmium yellow pigment particles depending on the synthesis method and chemical environment

A type of cadmium pigment	Type of environment and value of surface potential in mV		
	Acidic medium (5% v/v acetic acid), pH = 3	Slightly acidic medium (distilled water), pH = 6	Alkaline medium (0.1 M NaOH), pH = 9
P1	− 39.95	− 37.66	− 26.47
P1r	− 3.13	− 21.56	− 29.6
P2	− 20.19	− 27.39	− 32.08
P2r	− 9.89	− 9.78	− 24.32
P3	− 7.91	–[1]	− 37.73
P3r	− 14.59 − 4.75	− 24.43	− 35.86 − 20.03
P4	− 2.45	− 8.55	− 24.06
P4r	− 23.29	− 34.69	–[1]
P5	− 15.13	− 38.55	− 27.07
P5r	− 3.6	-– 18.74	− 37.75 − 20.68
P6	− 11.38	− 23.31	− 35.96 − 26.66
P7	− 16.93 − 4.11	− 29.99	− 34.45

[1]Measurement not possible due to rapid aggregation and sedimentation.

intensity reflect the influence of the precursor type and calcination on the structural order.

Electrokinetic potential of cadmium yellow pigment dispersions in different media

The electrokinetic behavior of cadmium yellow (CdS) pigments in aqueous environments was assessed through ζ potential measurements at pH 3, 6, and 9, representing acidic, near-neutral, and alkaline conditions, respectively. Table 2 summarizes the measured ζ potential values for pigments synthesized by different routes and subjected to drying or calcination.

All measured pigment particles exhibited negative ζ potential values, indicating a dominant anionic surface charge under the tested conditions. The absolute ζ values depended strongly on pH and thermal treatment. In acidic media, more negative potentials were generally observed, reflecting a higher density of protonable surface groups and stronger surface charge. In alkaline media, some pigments exhibited less negative potentials, suggesting changes in the protonation/deprotonation equilibrium or specific ion adsorption mechanisms. Rapid aggregation and sedimentation in certain systems prevented reliable ζ measurements, consistent with low colloidal stability.

Calcination led to significant changes in ζ values, associated with alterations in the surface chemistry and the number/type of active sites capable of ionization or adsorption. HR-XPS results indicate surface oxidation after thermal treatment (e.g., the appearance/increase of oxidized sulfur S(VI) and higher binding energy Cd species), which may modify the electrical double layer structure and thus influence ζ values. Consequently, we avoid assigning these changes to specific "dopant phases," focusing instead on surface chemical states.

The correlation between pigment surface structure and ζ potential was further evaluated using the Raman 2LO/1LO intensity ratio as an indicator of crystallinity and defect density. Across all pH conditions, higher Raman intensity generally corresponded to more positive ζ potentials, reflecting a more ordered structure and fewer surface defects. Acidic conditions promoted surface degradation of dried pigments, whereas calcination improved resistance. Neutral media resulted in a compromise between structural order and electrokinetic behavior, while alkaline conditions led to higher negative surface charge and increased reactivity, likely due to enhanced surface defects (see Fig. 2).

The ζ potential measurements indicate that the electrokinetic behavior of CdS pigments is strongly influenced by both the pH of the medium and thermal

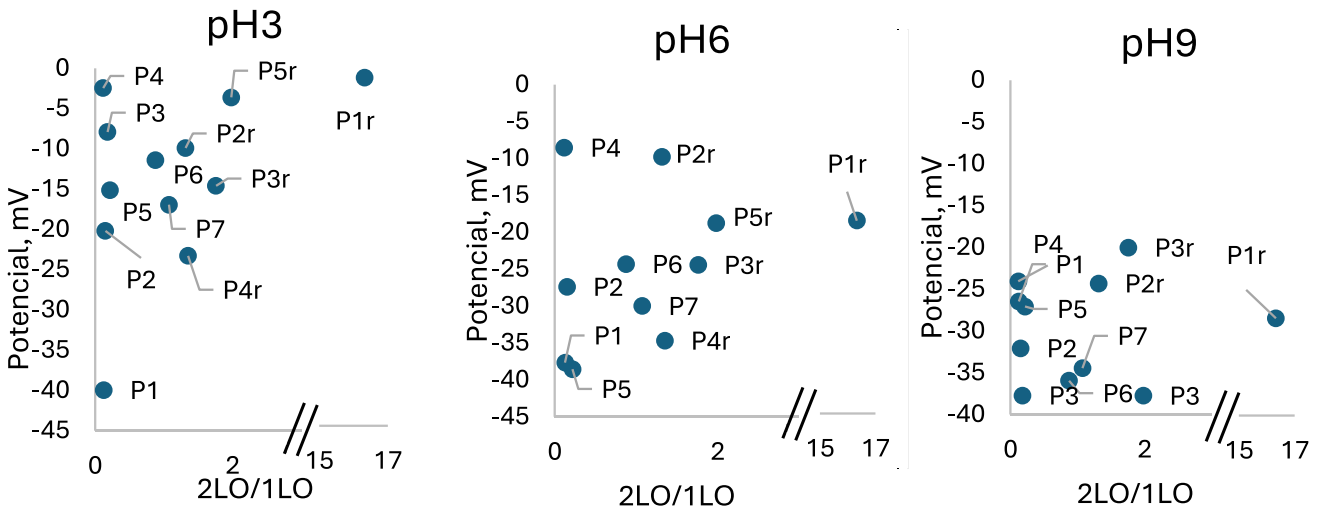

Figure 2 Relationship between the surface potential (ζ) of CdS pigment particles and the Raman 2LO/1LO intensity ratio in aqueous media at different pH values. Pigment types and compositions are listed in Table 1.

treatment. Calcined pigments show a reduced negative ζ potential, which may affect colloidal stability and chemical interactions. Higher negative ζ values in acidic environments suggest a greater surface charge density and potentially improved dispersion stability, whereas in alkaline media there is a tendency toward aggregation.

Overall, these results demonstrate that the electrokinetic behavior of CdS pigments is strongly influenced by synthesis route, thermal treatment, and surface chemistry. Combining ζ potential measurements with HR-XPS and Raman spectroscopy provides a comprehensive understanding of pigment surface properties, their colloidal stability, and potential performance in aqueous systems.

Electrokinetic potential and surface composition of pigment dispersions in different media

The electrokinetic potential of the pigment particles originated from their immersion in aqueous electrolyte solutions. At the solid–liquid interface, a thin layer was formed, in which ions from the solution and decomposition products of surface impurities were adsorbed. Measurements showed that in all investigated solutions, the electrokinetic potential of pigment particles had negative values, resulting from the adsorption of anions. Analysis of the raw materials used for pigment synthesis indicated that they could have originated from compounds containing elements such as oxygen, carbon, chlorine, and sulfur. To determine the chemical composition of elements present on the pigment surface, X-ray photoelectron spectroscopy (XPS) was used. Table 3 presents detailed surface atomic concentrations of the individual elements expressed in atomic percent. The table includes pigments after precipitation and drying as well as after calcination.

Table 3 Atomic concentration (at.%) of individual elements present on the surface of pigments after precipitation and drying, and after calcination

Pigment type and designation	Oxygen (O)	Carbon (C)	Chlorine (Cl)	Sulfur (S)
P1	12.72	7.07	6.34	30.48
P2	7.10	8.69	3.80	34.93
P3	36.83	9.23	–	16.95
P4	10.50	5.85	–	34.82
P5	18.69	3.91	–	3.56
P1r	25.75	1.84	7.63	15.71
P2r	27.46	17.39	9.81	16.65
P3r	44.83	6.18	–	20.94
P4r	40.23	10.73	–	21.49
P5r	55.38	6.47	–	14.04
P6	55.26	6.96	–	15.90
P7	16.01	9.67	–	32.95

Based on the data presented in Table 3, it can be inferred that the negative charge of the pigment particles is primarily associated with the presence of chloride, sulfite, sulfate, and carbonate anions. The value

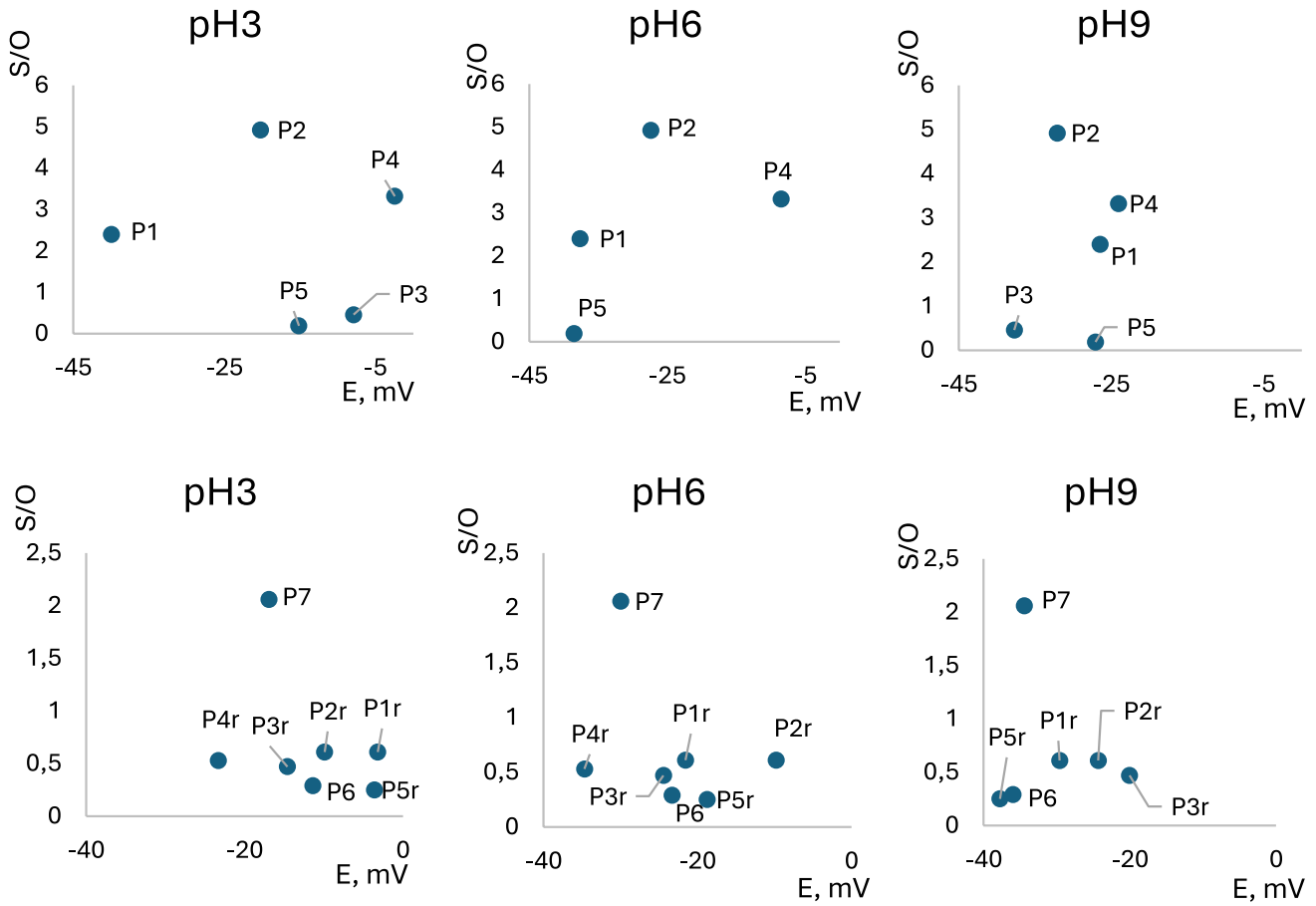

Figure 3 Dependencies of the S/O ratio in the resulting compounds on the surface of pigment particles after drying and roasting on their potential in environments with different concentrations of hydrogen ions. The type and compositions of pigments are given in Table 3

of the electrokinetic potential is mainly determined by anions containing sulfur and oxygen atoms, as these elements were present in the highest concentrations. In this case, the dominant anions were the sulfite anion (S/3O = 0.67) and the sulfate anion (S/4O = 0.50). Figure 3 shows the relationship between the S/O ratio for individual pigments and their electrokinetic potential. Both the pigments after precipitation and drying, as well as those after calcination, were taken into account.

Based on the data presented in Fig. 3, it can be concluded that at higher S/O ratios, the electrokinetic potential of pigment particles in the acidic environment became more negative, suggesting a greater presence of sulfite-type compounds. In contrast, in environments with pH 6 and 9, the relationship between potential and the S/O ratio was more complex. In these cases, an increased influence of the surface structure of pigment particles was observed, likely related to the presence of impurities such as CdO and $CdSO_4$. In the acidic environment, when the S/O ratio was very low (below 0.6), the pigment particles contained less sulfur, indicating a lower proportion of oxidized compounds such as oxides or sulfates. In the alkaline environment, adsorption processes involving ions such as OH^- occurred on the pigment surface, thereby influencing changes in the surface charge of the particles. In neutral and alkaline environments, the observed trend was often reversed. Some pigment samples, such as P5r and P6, exhibited highly negative electrokinetic potentials at low S/O ratios. Overall, it can be concluded that the type and amount of oxidized impurities—such as oxides, sulfites, sulfates, and carbonates—had a significant effect on the surface charge of pigment particles. A high S/O ratio in acidic conditions indicated a more sulfate-like surface character and a more negative electrokinetic potential. It was observed

that both dried and calcined pigment samples with a high S/O ratio showed a shift of the potential toward less negative values. Conversely, the calcination process led to a decrease in the S/O ratio and a shift of the potential toward more negative values. The hydrogen ion concentration in the aqueous environment had a pronounced influence on the electrokinetic potential of pigment particles. In all measurement series, a clear trend was observed: a higher S/O ratio corresponded to a less negative electrokinetic potential of the pigment particles.

High-resolution XPS (HR-XPS) analysis of the key core levels (S 2p, Cd 3d, O 1s) revealed that calcination induced significant changes in the surface chemistry of the pigments. In particular, the S 2p spectra showed the appearance or increased intensity of a component corresponding to oxidized sulfur (S(VI)) at binding energies of approximately 169.0–169.5 eV, which can be attributed to sulfate species on the pigment surface. Concurrently, the oxygen content in the outermost surface layer increased. The Cd 3d spectra exhibited a component at slightly higher binding energy, consistent with the presence of oxidized cadmium species (CdO or $Cd(OH)_2$-like phases), indicating enhanced chemical heterogeneity of the surface. These surface modifications were reflected in the ζ-potential measurements: pigments with higher S(VI) content and more oxidized Cd species generally showed more negative electrokinetic potentials, particularly in alkaline media. This relationship suggests that changes in surface chemistry, rather than specific crystalline phases, govern the structure of the electrical double layer and, consequently, the electrokinetic behavior and dispersion stability of CdS pigments.

Stability of pigment dispersions in different media

Sedimentation studies of pigments in various environments were carried out using a Turbiscan device. The tests consisted in determining the sedimentation curves of pigment particles in aqueous chemical media with precisely defined acidity. Figure 4 shows the sedimentation curves of pigments P1 and P1r in different aqueous environments as a function of time. The parameter used to describe the sedimentation rate of pigment particles was the Turbiscan Stability Index (TSI). This index represents the change in the intensity of transmitted and scattered light signals during the sedimentation process of pigment particles in an aqueous dispersion.

The sedimentation studies showed that the stability index (TSI) assumes different values depending on the type of environment. A low TSI value indicates a highly stable system, in which only slight changes in pigment particle size occur. In contrast, a high TSI value is associated with significant instability of the dispersion system, caused by the formation of large agglomerates of pigment particles. Figure 4 clearly shows the effect of the aqueous medium pH on the stability of pigments P1 and P1r. In the aqueous environment at pH 3, pigment P1r rapidly reached a high TSI value, which then stabilized and remained nearly constant. This indicated that the dispersion system underwent rapid destabilization. For pigment P1, the TSI value initially increased slowly and then more rapidly, suggesting the occurrence of pigment particle agglomeration and sedimentation processes within the dispersion system. In the aqueous medium with

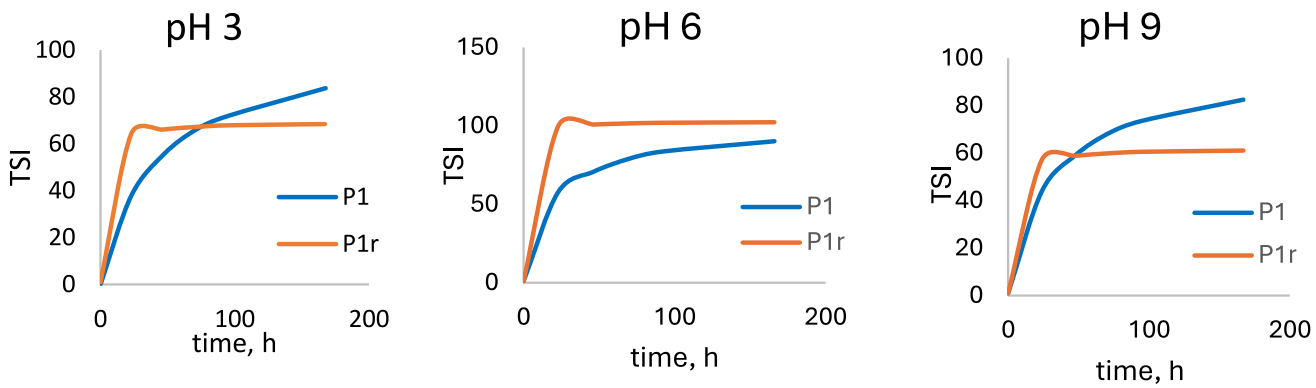

Figure 4 Dependence of the stability index of yellow cadmium pigment P1 and P1r on the sedimentation time in chemical environments with different acidity. The type and compositions of pigments are given in Table 1

pH 6, the dispersion of pigment P1 was highly stable, as the TSI value increased slowly and its final value remained very low. In this environment, the dispersion of pigment P1 was more stable than that of pigment P1r. In the medium with pH 9, the dispersion of pigment P1 initially exhibited a low TSI value. At a later stage, the TSI value increased, reaching a level comparable to that obtained for the P1r pigment dispersion. This phenomenon indicated pigment particle agglomeration and destabilization of the pigment dispersion in water.

For the sedimentation stability studies of the remaining pigment dispersions, similar dependencies of the TSI index on time were obtained. All the TSI–time curves could be described by an exponential equation of the form:

$$[\mathrm{TSI}] = A \cdot t^{b} \tag{7}$$

In Eq. (1), the constant "A" was closely related to the value of the TSI index. A higher value of constant "A" corresponded to a higher TSI value and, consequently, to greater instability of the dispersion system. The constant "b", on the other hand, represented the rate of change in the stability of the dispersion system. A higher value of constant "b" indicated a faster destabilization process. Table 4 presents the values of constants "A" and "b", determined from the analysis of the sedimentation curves, for all examined aqueous pigment dispersion systems.

The highest values of constant "A" in the aqueous medium at pH 3 were observed for pigments P7, P6, and P4r. This indicated that these pigments formed dispersions with the greatest instability. In the aqueous medium with pH 6, high values of constant "A" were obtained for pigments P1r, P7, and P2r, which clearly indicated the formation of unstable aqueous dispersions. In contrast, in the aqueous medium with pH 9, pigments P3r and P4r exhibited significantly lower values of constant "A", indicating the formation of stable dispersions. It can be concluded that the values of constant "A" for pigments after calcination were higher than those for pigments obtained by precipitation and drying. This suggests that the calcination process promotes dispersion instability. Exceptions were pigments P3r and P4r, which, in the aqueous medium at pH 9, exhibited low values of constant "A" and formed stable dispersion systems. The values of constant "b" ranged from 0.32 to 0.37. Dispersion systems with "b" values close to 0.37 were characterized by high instability, while those with values near 0.32 showed a very slow increase in the TSI index and greater stability of the aqueous dispersions formed. In general, it can be stated that in the acidic medium at pH 3, pigments P4r, P6, and P7 formed highly unstable dispersion systems. In the medium with pH 6, most pigments also formed unstable dispersions, whereas in the medium with pH 9, stable dispersions were formed by pigments P3r and P4r. Their stability was higher than in the media with pH 3 and 6. A high pH of the aqueous environment inhibited the sedimentation processes of pigment particles.

Table 4 Values of the constants "A" and "b" from Eq. (1), describing the sedimentation process of pigments in aqueous media with different pH levels

Type of pigment	Acidic aqueous medium (pH 3)		Near-neutral aqueous medium (pH 6)		Aqueous alkaline medium (pH 9)	
	Parameter A	Parameter b	Parameter A	Parameter b	Parameter A	Parameter b
P1	2.9917	0.492	17.614	0.3477	15.658	0.3358
P1r	16.322	0.3343	21.604	0.3675	15.065	0.3251
P2	12.09	0.3139	12.79	0.3131	14.925	0.3309
P2r	22.208	0.3709	18.222	0.3474	16.781	0.338
P3	13.486	0.3241	14.632	0.3265	17.681	0.3454
P3r	21.252	0.3661	18.974	0.352	7.3993	0.3308
P4	18.963	0.3556	13.478	0.3263	13.539	0.3275
P4r	21.306	0.3663	18.266	0.3478	8.278	0.2544
P5	14.163	0.3304	14.53	0.329	13.86	0.3219
P5r	21.109	0.3654	18.221	0.3473	17.282	0.3414
P6	21.33	0.3666	16.85	0.3353	17.319	0.3419
P7	23.137	0.3772	21.146	0.3665	18.304	0.3504

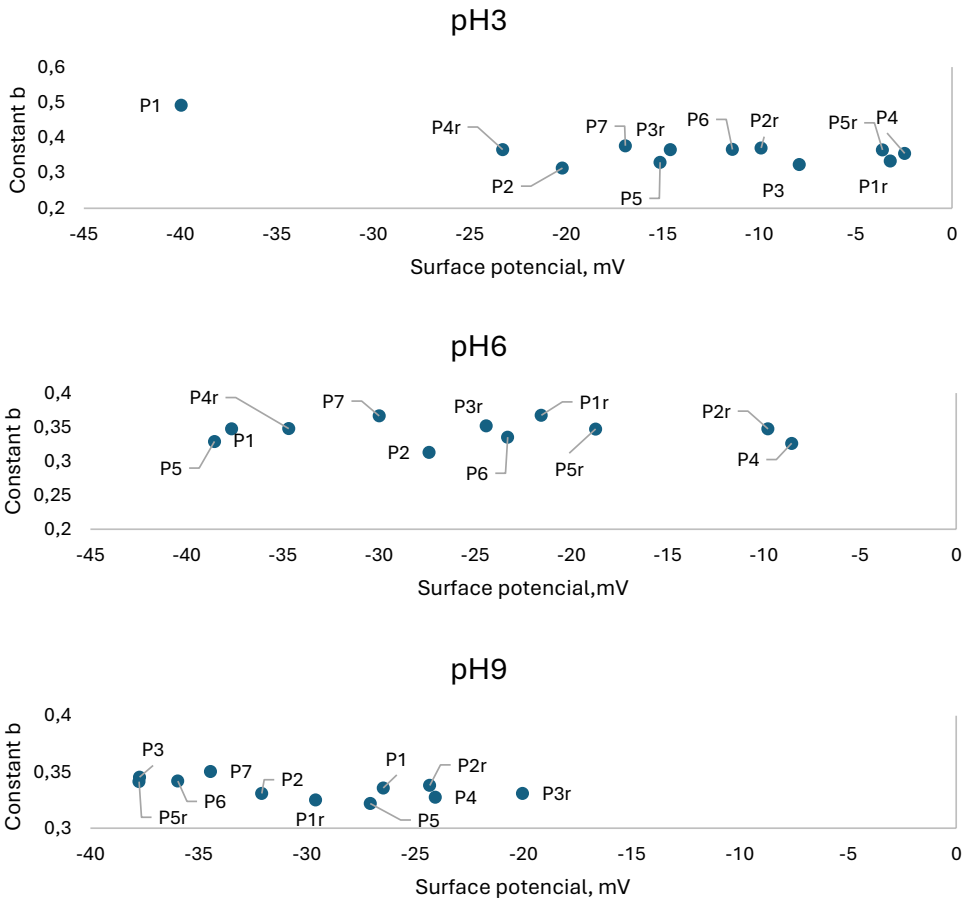

Figure 5 Dependencies of the settling rate constant "*b*" of pigment particles after precipitation and drying and after roasting on the value of their surface potential. The type and compositions of pigments are given in Table 1

Pigments after calcination formed dispersion systems with lower stability.

The data presented in Fig. 5 indicate that in the acidic medium (pH 3), the surface potential of pigment particles shifted toward less negative values, particularly for pigments after calcination. At the same time, the values of constant "*b*" for the calcined pigments generally increased. This phenomenon suggests a faster sedimentation of pigment particles in strongly acidic environments. For example, in the case of pigments P1 and P1r, the surface potential of P1r particles was less negative, indicating a greater tendency of these particles to aggregate. Similar relationships were observed for the other pigments as well. In general, it can be concluded that the calcination process promotes an increase in the sedimentation rate constant "*b*" of pigment particles in strongly acidic media and enhances their tendency to aggregate. In the medium with pH 6, an increase in the value of the constant "*b*" was also observed, indicating a greater propensity of pigment particles to aggregate. In contrast, in the medium with pH 9, the values of this constant ranged from 0.30 to 0.36, suggesting slower sedimentation of pigment particles compared to those in media with pH 3 and 6. In this alkaline environment, the dispersion properties of the pigments were very similar to each other. The study clearly demonstrated the influence of both the pH of the medium and the pigment calcination process on the surface properties of the pigments and their tendency to aggregate. The highest dispersion stability of pigment particles was recorded in the medium with pH 3, where their surface potentials reached the most negative values. As the pH increased, the surface potentials became less negative, which clearly indicated a reduction in the stability of the aqueous dispersions. At the same time, the range of the sedimentation rate constant "*b*" gradually narrowed. In the alkaline medium (pH 9), all pigments exhibited a similar rate of TSI increase, indicating a more uniform course of the pigment particle aggregation processes.

Table 5 Quantitative correlation analysis between Raman 2LO/1LO ratio, zeta potential (ζ), and sedimentation stability parameters (A, b) at pH 3, 6, and 9

pH	Variable pair	*N*	Pearson *r*	*p*-value	Spearman ρ	*p*-value
3	2LO/1LO versus ζ	12	0.356	0.26	0.217	0.50
3	2LO/1LO versus *A*	12	0.051	0.88	0.483	0.11
3	2LO/1LO versus *b*	12	− 0.197	0.54	0.105	0.75
3	ζ versus *A*	12	0.595	0.041	0.112	0.73
3	ζ versus *b*	12	− 0.690	0.013	− 0.349	0.27
6	2LO/1LO versus ζ	11	0.148	0.66	0.064	0.85
6	2LO/1LO versus *A*	12	0.580	0.048	0.741	0.0058
6	2LO/1LO vs *b*	12	0.609	0.035	0.699	0.011
6	ζ versus *A*	11	− 0.042	0.90	0.018	0.96
6	ζ versus *b*	11	− 0.044	0.90	− 0.118	0.73
9	2LO/1LO versus ζ	11	0.018	0.96	− 0.295	0.38
9	2LO/1LO versus *A*	12	− 0.003	0.99	− 0.028	0.93
9	2LO/1LO versus *b*	12	− 0.064	0.84	− 0.105	0.75
9	ζ versus *A*	11	− 0.770	0.0057	− 0.764	0.0063
9	ζ versus *b*	11	− 0.613	0.045	− 0.618	0.042

N = number of data points used for the correlation; *N* varies due to missing ζ-potential values

Correlation between chemical composition, zeta potential and dispersion stability

To quantitatively evaluate the relationships between Raman metrics, electrokinetic properties, and dispersion stability, correlation analysis was performed between the Raman 2LO/1LO ratio, ζ-potential, and Turbiscan-derived stability parameters (A and b), separately for pH 3, 6, and 9 (Table 5). The 2LO/1LO–ζ correlations were weak and statistically non-significant across all pH conditions, indicating that the Raman ratio alone is not a global predictor of ζ-potential for the entire sample set. In contrast, ζ-potential exhibited significant correlations with stability parameters in acidic and alkaline media (ζ–b at pH 3; ζ–A and ζ–b at pH 9), supporting the role of electrokinetic effects in controlling destabilization kinetics. At pH 6, moderate and statistically significant correlations were found between 2LO/1LO and both A and b, suggesting that under near-neutral conditions structural/crystallinity-related Raman metrics may be more directly linked to sedimentation behavior than ζ alone.

Discussion

The qualitative composition of the studied pigments was confirmed by Raman spectroscopy, revealing that the main component of each pigment was yellow cadmium sulfide. In addition, by-products originating from both the pigment synthesis and calcination processes were present. The temperature at which calcination was conducted influenced the crystallinity and structural order of the pigment particles, which in turn affected their electrokinetic properties.

Measurements of surface potential in aqueous dispersions of different pH values highlighted the role of electrokinetic properties in pigment stability. All pigment particles, whether after precipitation and drying or after calcination, exhibited negative surface potentials in aqueous media. The most negative potentials were observed under strongly acidic conditions, while the potentials became less negative as the medium approached neutrality. This behavior was closely linked to the chemical composition of the pigment surfaces, particularly the presence of oxygen- and sulfur-containing species detected by X-ray photoelectron spectroscopy (XPS). Calcination reduced the number of active adsorption sites, resulting in less negative potentials and a modified surface charge distribution.

Raman spectroscopy provided insight into the structural characteristics of the pigment surfaces through the 2LO/1LO ratio. To quantitatively link structural, electrokinetic, and sedimentation properties, correlation analysis was performed separately for pH 3, 6, and 9 between the Raman 2LO/1LO ratio, ζ-potential, and Turbiscan-derived parameters (A and b).

Across all pH values, the correlation between 2LO/1LO and ζ-potential was weak and not

statistically significant, indicating that the Raman ratio alone is not a universal predictor of electrokinetic behavior.

ζ-potential showed significant correlations with sedimentation parameters in acidic and alkaline media (ζ–b at pH 3; ζ–A and ζ–b at pH 9), highlighting the role of surface charge in controlling destabilization kinetics. Stronger negative potentials generally corresponded to slower sedimentation rates, confirming that electrostatic repulsion contributes to dispersion stability.

At near-neutral pH (6), moderate and statistically significant correlations were observed between the Raman 2LO/1LO ratio and both A and b, suggesting that under near-neutral conditions structural/crystallinity-related Raman metrics may be more directly linked to sedimentation behavior than ζ alone.

These findings indicate that dispersion stability is controlled by a combination of electrostatic and structural factors, with their relative contributions depending on the pH of the medium. Electrokinetic effects dominate in strongly acidic and alkaline environments, while structural and crystallinity-related properties exert a stronger influence under near-neutral conditions.

Conclusion

The stability of cadmium sulfide pigment dispersions depends on both electrostatic and structural factors, with their relative importance being dependent on the pH of the medium. The ζ-potential plays a key role in sedimentation behavior in strongly acidic and alkaline environments, with more negative potentials corresponding to slower sedimentation and higher dispersion stability. Under near-neutral conditions, structural properties and particle crystallinity, reflected by the Raman 2LO/1LO ratio, are more directly associated with sedimentation behavior than ζ-potential alone. Calcination modifies the surface chemistry and particle structure, leading to a reduction in the number of active adsorption sites, less negative ζ-potentials, and faster sedimentation. Overall, dispersions of precipitated and dried pigments are more stable than those of calcined pigments, and acidic environments promote greater dispersion stability than alkaline media. Integrated analysis of Raman spectroscopy data, ζ-potential measurements, and Turbiscan-derived sedimentation parameters provides a comprehensive understanding of dispersion behavior and enables optimization of pigment synthesis and post-processing to achieve desired stability and functional properties.

Author contributions

Magdalena Tworek: Conceptualization, Methodology, Investigation, Writing–Reviewing and Editing Visualization Edwin Makarewicz: Writing–Original draft preparation, Conceptualization Magdalena Osiał: Investigation, Validation Joanna Kowalik: Investigation Magdalena Warczak: Investigation.

Funding

This research did not receive any specific grant from funding agencies in the public, commercial, or not-for-profit sectors.

Data availability

Data available on request from the authors.

Declarations

Conflict of interest Not Applicable.

Ethical approval Ethical approval was waived for this study because no patients' data were reported.

References

[1] Pfaff G (2020) Inorganic pigments. De Gruyter
[2] Ahmed G, Metin A, Kubra G, Sadi GM (2022) Dyes and pigments, Springer Nature
[3] Logvinenko AD, Levin VL (2022) Fundations of colour science–from colorimetry to perception. John Wiley and Sons Ltd

[4] Blecher S (2024) Contemporary color, theory and use. Taylor and Francis Ltd, London
[5] Goldsmith I (2024) Colour theory for artists, Octopus Publishing Group
[6] Pochapski DJ, Santos CC, Leite GW, Pulcinelli SH, Santilli CV (2021) Zeta potential and colloidal stability predictions for inorganic nanoparticle dispersions: effects of experimental conditions and electrokinetic models on the interpretation of results. Langmuir 37(45):13379–13389. https://doi.org/10.1021/acs.langmuir.1c02056
[7] Nasser A (2020) Chemistry and technology of natural and synthetic dyes and pigments, Intechopen
[8] Ingo K (2022) Handbook Of colorants chemistry. De Gruyter
[9] Eastaugh N, Walsh V, Chaplin T (2008) Pigment compedium. Taylor and Francis Ltd
[10] Wang F, Xue Y, Lu B, Luo H, Zhu J (2019) Fabrication and characterization of angle-independent structurally colored films based on CdS@SiO_2 nanospheres. Langmuir 35(14):4918–4926. https://doi.org/10.1021/acs.langmuir.8b04193
[11] Liu H, Gao H, Long M, Fu H, Alvarez PJJ, Li Q, Zheng S, Qu X, Zhu D (2017) Sunlight promotes fast release of hazardous cadmium from widely-used commercial cadmium pigment. Environ Sci Technol 51(12):6877–6886. https://doi.org/10.1021/acs.est.7b00654
[12] Turner A (2019) Cadmium pigments in consumer products and their health risks. Sci Total Environ 657:1409–1418. https://doi.org/10.1016/j.scitotenv.2018.12.096
[13] Thoury M, Delaney J, Rene de la Rie E, Palmer M, Morales K, Krueger J (2011) Near-infrared luminescence of cadmium pigments: in situ identification and mapping in paintings. Appl Spectrosc 65:939–951
[14] Monico L, Rosi F, Vivani R et al (2022) Deeper insights into the photoluminescence properties and (photo)chemical reactivity of cadmium red ($CdS_{1-x}Se_x$) paints in renowned twentieth century paintings by state-of-the-art investigations at multiple length scales. Eur Phys J Plus 137:311. https://doi.org/10.1140/epjp/s13360-022-02447-7
[15] Ghirardello M, Otera V, Comelli D, Toniolo L, Dellasega D, Nessi L, Conton M et al (2021) An investigation into the synthesis of cadmium sulfide pigments for a better understanding of their reactivity in artworks. Dyes Pigm 186:108998. https://doi.org/10.1016/j.dyepig.2020.108998
[16] Bandow N, Simon FG (2016) Significance of cadmium from artists' paints to agricultural soil and the food chain. Environ Sci Eur 28:12. https://doi.org/10.1186/s12302-016-0077-6
[17] Haisel D, Cyrusova T, Vanek T, Podlipna R (2019) The effect of nanoparticles on the photosynthetic pigments in cadmium—zinc interactions. Environ Sci Pollut Res Int 26:4147–4151. https://doi.org/10.1007/s11356-018-04060-7
[18] Yang S, Wei P, Wang J, Tan Y, Qu X (2023) Impacts of dissolved organic matter on the aggregation and photodissolution of cadmium pigment nanoparticles in aquatic systems. Sci Total Environ 865:161313. https://doi.org/10.1016/j.scitotenv.2022.161313
[19] Pouyet E, Cotte P, Foyard B et al (2015) 2D X-ray and FTIR micro-analysis of the degradation of cadmium yellow pigment in paintings of Henri Matisse. Appl Phys 121:967–980. https://doi.org/10.1007/s00339-015-9239-4
[20] Van der Snickt G, Dik J, Cotte M et al (2009) Characterization of a degraded cadmium yellow (CdS) pigment in an oil painting by means of synchrotron radiation based X-ray techniques. Anal Chem 81(7):2600–2610. https://doi.org/10.1021/AC802518Z
[21] Liu H, Zhang L, Zhao J, Zhou Z, Luo Y (2017) Sunlight promotes fast release of hazardous cadmium from widely used commercial cadmium pigments. Environ Sci Technol 51(10):5682–5690. https://doi.org/10.1021/acs.est.7b00764
[22] Pisu F, Carbonaro C, Ricci P, Porcu S (2014) Electrochemical photodegradation study of semiconductor pigments: influence of environmental parameters. Heritage Basel 7(5):2426–2443. https://doi.org/10.1021/ac502303z
[23] Wei W, Wu C, Fang Q, Zhao Z, Su X (2023) Beyond cadmium yellow: CdS photonic crystal pigments with vivid structural colors. J Mater Chem C 11:12667–12674. https://doi.org/10.1039/D3TC01987J
[24] Scofield JH (1976) Hartree-slater subshell photoionization cross-section at 1254 and 1487 eV. J Electron Spectros Relat Phenom 8:129–137
[25] Moulder JF, Stickle WF, Sobol PE, Bomben KD (1992) Handbook of X-ray photoelectron spectroscopy. Perkin-Elmer Corp., Eden Prairie
[26] Maticiuc N, Katerski A, Danilson M, Krunks M, Hiie J (2017) XPS study of OH impurity in solution processed CdS thin films. Sol Energy Mater Sol Cells 160:211–216
[27] Marychurch M, Morris GC (1985) X-ray photoelectron spectra of crystal and thin film cadmium sulphide. Surf Sci 154:L251–L254
[28] Zemlyanov DY, Savinova E, Scheybal A, Doblhofer K, Schögl R (1998) XPS observation of OH groups incorporated in an Ag(111) electrode. Surf Sci 418:441–456. https://doi.org/10.1016/S0039-6028(98)00728-6

[29] Manca ML, Matricardi P, Cencetti C, Peris JE, Melis V, Carbone C, Escribano E, Zaru M, Fadda AM, Manconi M (2016) Combination of argan oil and phospholipids for the development of an effective liposomelike formulation able to improve skin hydration and allantoin dermal delivery. Int J Pharm 505:204–211. https://doi.org/10.1016/j.ijpharm.2016.04.008